Numerical study of step forward swept angle effects on the hydrodynamic performance of a planing hull

Hadi Nourghasemi, Mohammad Bakhtiari, Hassan Ghassemi⊠

Amirkabir University of Technology, Department of Maritime Engineering
Hafez Ave, No. 424, P.O. Box 15875-4413, Tehran, Iran
email: gasemi@aut.ac.ir
⊠ corresponding author

Abstract

One of the most effective methods to diminish the drag of a planing craft is to use a step at the bottom of the hull. A stepped hull causes a reduction of the wetted area and, as a result, a decrease in the drag. The step may be designed as a straight line through the entire width of the hull or may be V-shaped with a forward or backward swept angle. In this paper, the effects of the step forward swept angle on the hydrodynamic performance of a hard chine planing vessel are investigated by finite volume method (FVM). Reynolds-Averaged Navier Stokes (RANS) equations with a standard k-ε turbulence model coupled with volume of fluid (VOF) equations are solved in order to simulate a transient turbulent free surface flow around the hull with the help of Ansys CFX software. In order to predict hull motions, equations of rigid body motions for two degrees of freedom (2-DOF) are coupled with fluid flow governing equations. To validate the presented numerical model, first the numerical results are compared with available experimental data, and then the obtained numerical results of the drag, dynamic trim, sinkage, wetted keel length, wetted chine length, pressure distribution on the hull, wetted surface and wake profile at different Froude numbers and step angles are presented and discussed.

Introduction

In recent decades, researchers have made many attempts to reduce drag and thus increase the speed of planing vessels by changing hull form. Various configurations, such as chine, step, strake, pad and tunnels, have been used. Using a step at the bottom of the hull is known to be one of the most effective of these methods. Steps may be designed as a straight line through the entire width of the hull (this type being less common today) or may be V-shaped with a forward or backward swept angle (Figure 1). They have large apertures on the outboard side of the hull to allow air to be sucked down into, and ventilate, the step. In general, a speed rise of about 10–15% can be expected from a stepped hull over a non-stepped hull with the same power. The idea behind a stepped hull is to reduce the wetted surface by allowing the hull to plane on two or three small wetted planing surfaces rather than one large one. Since the lift is spread across several surfaces along the hull, the longitudinal stability becomes very large. Despite these advantages, there is some danger due to the closing of the air by waves. When
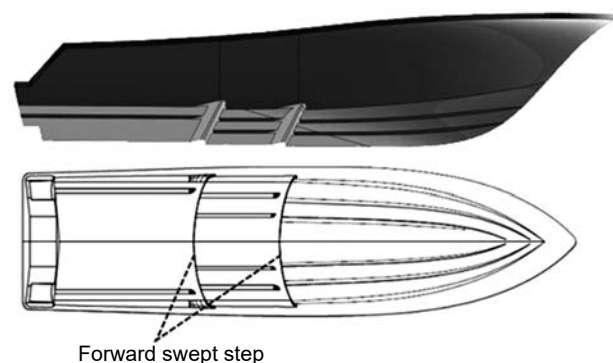

Figure 1. A view of a planing hull with two forward swept steps

the air supply is lost, a reverse flow occurs behind the step, causing an excessive increase in drag. The speed rapidly drops and the craft will turn suddenly, and possibly even capsize. To avoid this problem, air is often sucked through openings well above the waterline, or may be supplied through tubes at deck level.

To date, studies on the hydrodynamics of planing hulls have mainly concentrated on the simple mono-hull, that is, one without a step. A comprehensive contribution was made to the understanding and modelling of planing craft by (Savitsky, 1964). He developed regression formulas based on prismatic hull form model tests to estimate the hydrodynamic forces acting on planing craft. The effect of the whisker spray was investigated at the bow and on the drag (Savitsky, DeLorme & Datla, 2007). The hydrodynamic characteristics of planing surfaces were studied at steady state by the CFD method and the results obtained were compared with experimental results (Brizzolara & Serra, 2007). A computer code was developed based on the boundary element method for hydrodynamic analysis of planing and non-planing hulls (Ghassemi & Ghiasi, 2008). The results of the application of this code for hydrodynamic analysis of planing vessels were released (Ghassemi & Yumin, 2008; Kohansal, Ghassemi & Ghiasi, 2010; Kohansal & Ghassemi, 2010). The Fridsma planing hull in six degrees of freedom model was analysed by using the finite element method (Akkerman et al., 2012). In the same year, the hydrodynamic performances of a planing vessel were investigated by the CFD method based on RANS equations (Yumin et al., 2012). The forces acting on a multi-hull tunnel vessel were calculated in two degrees of freedom using the CFD method (Ghassabzadeh & Ghassemi, 2014). A systematic series of model tests was carried out to determine the effect of forward speed on hydrodynamic derivatives of a monohull planing craft (Kazerooni & Seif, 2017).

More recently, due to market needs and in order to make the stepped planing hull more efficient, marine researchers have devoted much effort to exploring it numerically and experimentally. A number of contributions on the planing stepped hull have been made over the past ten years. A mathematical model was developed for the prediction of planing hulls with a transverse step (Svahn, 2009). Extensive model tests were carried out to present a mathematical model to define the stern wake profile of prismatic planing hulls (Savitsky & Morabito, 2010). A series of high speed hard chine planing hulls were studied experimentally, with and without a step (Taunton, Hudson & Shenoi, 2010). The performance of a stepped planing hull was investigated by numerical simulation of non-linear flow on a 2D body (Garland & Maki, 2012). Numerical simulations of a hard chine planing hull were performed in two cases, with and without a step, in calm water, and the effects of the step on the hydrodynamic performance of a planing hull were studied (Veysi et al., 2014). The results of steady state simulations of flow around a stepped planing vessel were presented by (Bakhtiari, Veysi & Ghassemi, 2016).

In this paper, the effects of the step forward swept angle on the hydrodynamic performance of a hard chine planing hull are investigated by the numerical method of finite volume. For this purpose, the transient turbulent free surface flow around the hull is simulated by using RANS equations with a standard k-ε turbulence model coupled with VOF equations, with the help of Ansys CFX software. Also, equations of rigid body motions in two degrees of freedom are coupled with fluid flow governing equations in order to calculate the dynamic trim and sinkage of the hull. To validate the presented numerical model, first the numerical results for a zero-degree step angle are compared with experimental ones for different Froude numbers. Then, the calculated numerical results for drag, dynamic trim, sinkage, wetted keel length, wetted chine length, wetted surface and pressure distribution on the hull are presented for four different step forward swept angles, and the effects of these angles on hydrodynamic performance are discussed.

Governing equations

In order to predict the hydrodynamics of a planing vessel in calm water, the hull is considered as a rigid body with two degrees of freedom of heave and pitch, and simulations are carried out in a transient state. Therefore, the governing equations of turbulent free surface flow need to be solved in a coupled manner with equations of rigid body motions in two degrees of freedom.

Governing equations of fluid flow

The governing equations of fluid flow include the continuity equation and Navier-Stokes equation. After applying Reynolds averaging method, the RANS equations are obtained as follows:

$$\frac{\partial \rho}{\partial t} + \frac{\partial}{\partial x_i}\left(\rho\, u_j\right) = 0 \qquad (1)$$

$$\frac{\partial \rho u_j}{\partial t} + \frac{\partial}{\partial x_j}\left(\rho u_i u_j\right) =$$

$$= -\frac{\partial P}{\partial x_i} + \frac{\partial}{\partial x_j}\left(\tau_{ij} - \rho \overline{u_i' u_j'}\right) + g_i \qquad (2)$$

where: u, P and g are velocity, pressure and gravity respectively. $\rho \overline{u_i' u_j'}$ represents Reynolds stresses.

According to turbulence viscosity theory, which relates Reynolds stresses to velocity gradients, Eq. (2) can be written as:

$$\frac{\partial \rho u_i}{\partial t} + \frac{\partial}{\partial x_j}\left(\rho u_i u_j\right) =$$

$$= -\frac{\partial P}{\partial x_i} + \frac{\partial}{\partial x_j}\left[\mu_{\mathrm{eff}}\left(\frac{\partial u_i}{\partial x_j} + \frac{\partial u_j}{\partial x_i}\right)\right] + g_i \qquad (3)$$

where: μ_{eff} is effective viscosity and defined as:

$$\mu_{\mathrm{eff}} = \mu + \mu_t \qquad (4)$$

In order to model turbulence, the two-equations k-ε model is implemented, where k is turbulence kinetic energy and ε is turbulence dissipation rate. Then, the turbulent viscosity is calculated by the following equation:

$$\mu_t = C_\mu \rho \frac{k^2}{\varepsilon} \qquad (5)$$

where: C_μ is a constant. k and ε are calculated from the following transport equations:

$$\frac{\partial(\rho k)}{\partial t} + \frac{\partial}{\partial x_j}\left(\rho u_j k\right) =$$

$$= \frac{\partial}{\partial x_j}\left[\left(\mu + \frac{\mu_t}{\sigma_k}\right)\frac{\partial k}{\partial x_j}\right] + p_k - \rho\varepsilon \qquad (6)$$

$$\frac{\partial(\rho\varepsilon)}{\partial t} + \frac{\partial}{\partial x_j}\left(\rho u_j \varepsilon\right) =$$

$$= \frac{\partial}{\partial x_j}\left[\left(\mu + \frac{\mu_t}{\sigma_\varepsilon}\right)\frac{\partial\varepsilon}{\partial x_j}\right] + \frac{\varepsilon}{k}\left(C_{\varepsilon 1}p_k - C_{\varepsilon 2}\rho\varepsilon\right) \quad (7)$$

where: σ_k, $C_{\varepsilon 2}$ and $C_{\varepsilon 1}$ are constants, and p_k is turbulence production due to viscous forces.

Here, the volume of fluid (VOF) model is used to capture the air and water interface. In this case, the following transfer equation is solved to calculate the volume ratio of the two phases:

$$\frac{\partial\alpha}{\partial t} + \vec{\nabla}\cdot\left(\alpha\vec{u}\right) = 0 \qquad (8)$$

If $\alpha = 0$, the computational cell is inside the air, and if $\alpha = 1$, it is inside the water. $0 < \alpha < 1$ indicates that the cell is located at the free surface.

In the VOF model, effective density and viscosity inside each computational cell are used in Navier-Stokes equations, as follows:

$$\rho_{\mathrm{eff}} = \alpha\rho_{\mathrm{air}} + \left(1 - \alpha\right)\rho_{\mathrm{water}} \qquad (9)$$

$$v_{\mathrm{eff}} = \alpha v_{\mathrm{air}} + \left(1 - \alpha\right)v_{\mathrm{water}} \qquad (10)$$

Equations of motion for rigid body

The transitional motion equation of centre of gravity for a rigid body is stated as:

$$m\ddot{X}_G = \sum F_{\mathrm{ext}} \qquad (11)$$

where: $\ddot{X}_G$ is transitional acceleration tensor, and m is the mass of the body.

The rotational motion equations about the centre of gravity can be written as:

$$I\ddot{\theta}_G = \sum M_{\mathrm{ext}} \qquad (12)$$

where: $\ddot{\theta}_G$ is angular acceleration tensor, and I is the moment of inertia tensor.

In Eqs (11) and (12), the external forces and moments include the weight of the vessel and those exerted by the fluid.

In this study, equations of motion are solved in two degrees of freedom, including one transitional equation along the z-axis for heave and one rotational equation around the y-axis for pitch. The value of mass and pitch moment of inertia are 19.94 kg and 1.27 kg·m^2, respectively.

Solution domain and boundary conditions

The present study is carried out on a hard chine stepped planing vessel. This model, named C1, was tested at the University of Southampton and its experimental results are available for public use (Taunton et al., 2010). The specifications of this model are presented in Table 1 and a sketch of the model is shown in Figure 2.

Flow around the vessel can be assumed to be symmetrical with respect to the centre plane of the hull. Therefore, the solution domain is reduced to half the full domain. The distances of domain boundaries from the hull are determined in such a way that applying correct boundary conditions will be possible. Solution domains with applied boundary conditions are shown in Figure 3.

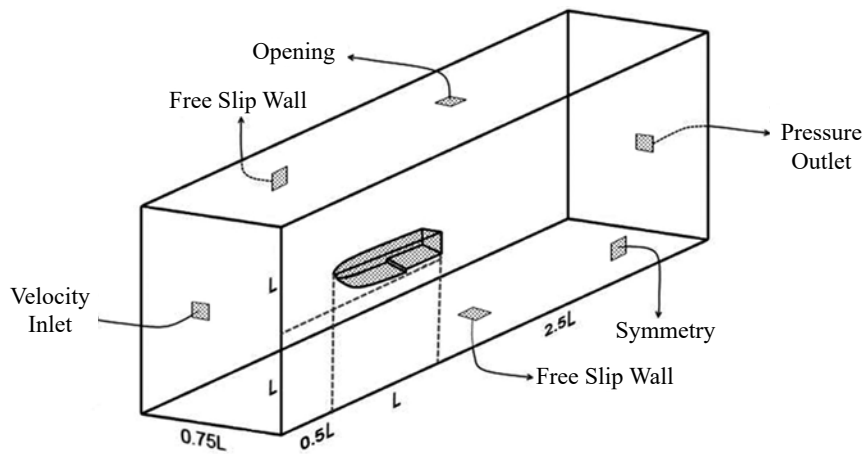**Figure 2. The sketch of the C1 stepped planing hull**

Figure 3. Solution domain and boundary conditions

Table 1. Model specifications

Parameter	Value
Length overall (m)	2
Breadth (m)	0.46
Draft (m)	0.09
Deadrise angle (degree)	22.5
Distance of the step from transom (m)	0.62
Height of step (m)	0.02
Mass (kg)	19.94
Pitch moment of inertia (kg·m^2)	1.27
Longitudinal distance of centre of gravity from transom (m)	0.742
Vertical distance of centre of gravity from keel (m)	0.099

Domain discretisation

The most important procedure in a numerical analysis is computational grid generation. The grid type and size of elements have great influence on the accuracy and convergence of solutions. Due to the complex geometry of the solution domain, an unstructured mesh including tetrahedral cells is used to discrete the domain. Because of large velocity gradients in wall-normal direction, an inflation layer mesh with high resolution is applied inside the boundary layer region of the flow. In layer mesh generation, the y^+ plus value and the number of computational nodes inside the boundary layer are very important and depend heavily on the selected turbulence model. In this research, the k-ε turbulence model with

$y^+ = 50$ is considered. There are approximately twenty layers inside the boundary layer. In order to better approximate the curvatures and sharp corners, the size of elements on the hull surface is fine enough. Moreover, the size of cells is decreased within two other regions where large gradients of solution variables are expected. The first region is around the free
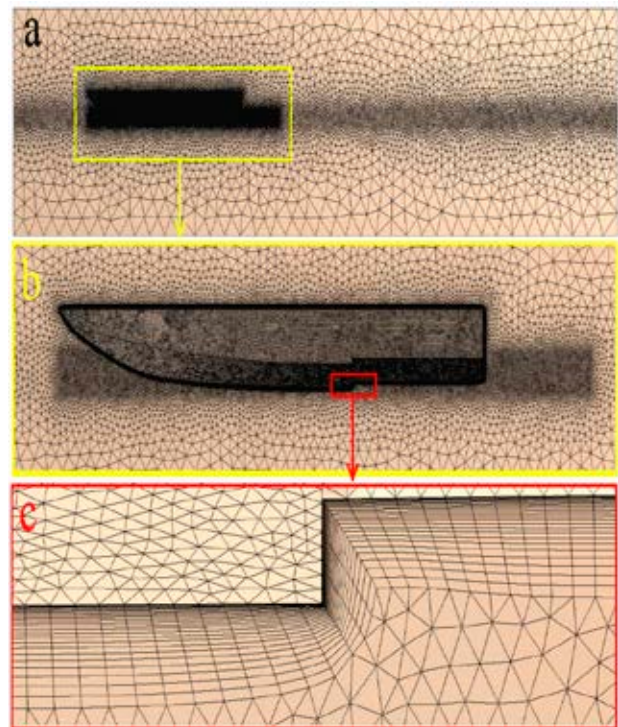

Figure 4. Computational grid around the hull, a) Full domain, b) Near field domain, c) Step region
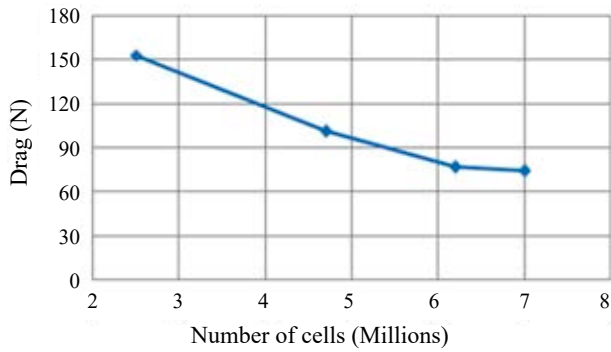
Figure 5. Mesh independency diagram for FnL = 3.34

surface, and the second is a part of the first region near the hull in which flow separation from chine, step and water spray occurs. The computational grid generated around the hull is shown in Figure 4.

In this paper, the dynamic mesh method is used for time-dependent analysis. In this method, the computational grid is updated with the hull movement at each time step. In order to prevent deformation of the inflation layer mesh inside the boundary layer,

mesh rigidity is applied to a distance of 30 mm from the hull so there is no deformation in the boundary layer mesh with the hull movement in time.

To evaluate the mesh independency of the obtained solution, computations were carried out in computational grids of different cell numbers for zero step forward swept angle. For instance, the variations of drag in terms of the number of cells for the Froude number 3.34 are shown in Figure 5.

Validation of numerical model

In this section, the numerical results obtained for zero-degree angle of step are presented and validated against experimental results. The stepped hull model studied in this paper was tested by Taunton et al. for zero-degree angle (Taunton et al., 2010), and the experimental results of wetted keel length (Lk), wetted chine length (Lc), dynamic sinkage (Zv), dynamic trim (θv) and drag force were presented. Numerical results of Lk, Lc, Zv, θv and drag for

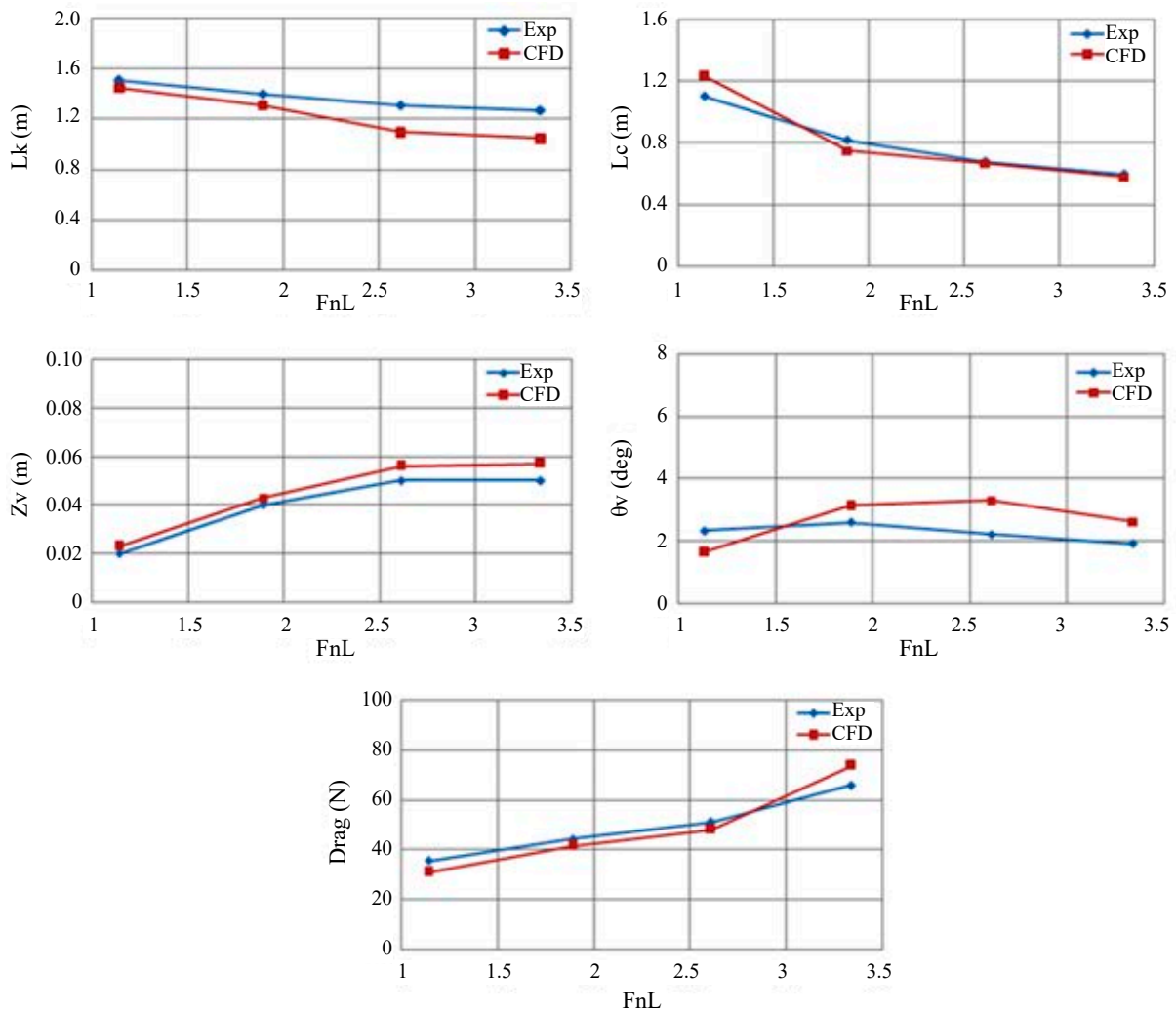**Figure 6. Comparison between numerical and experimental results for Lk, Lc, Zv, θv and drag at different Froude numbers**
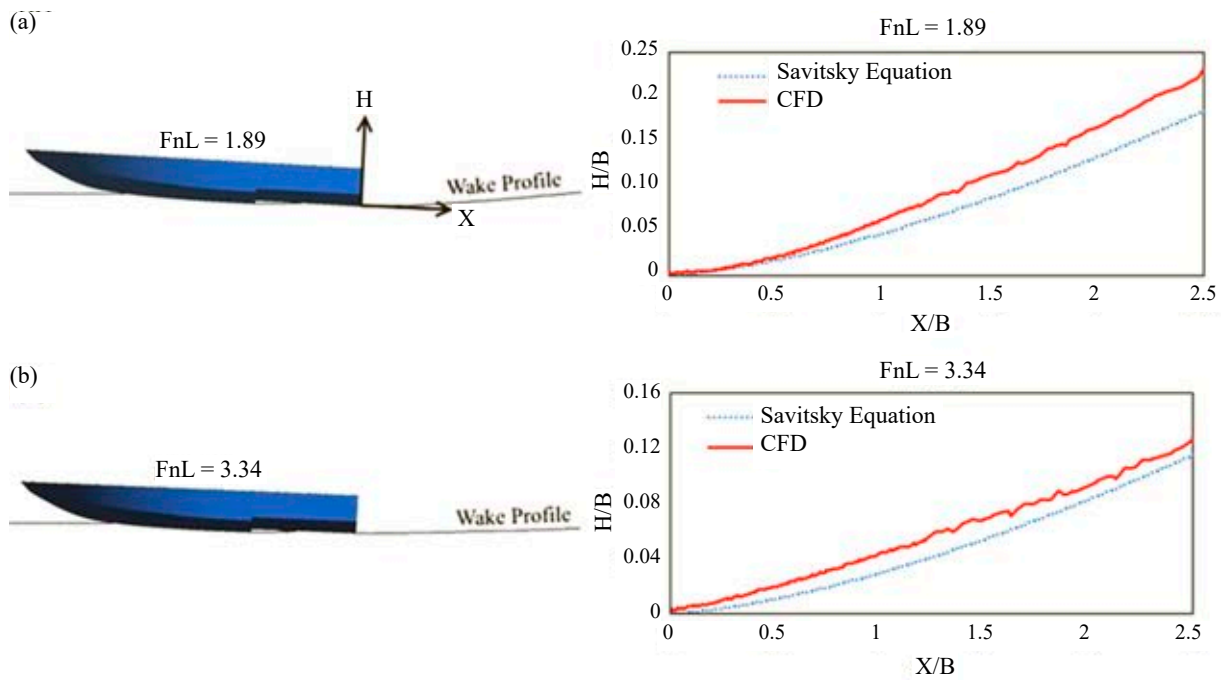
(a)

(b)

Figure 7. Comparison between the numerical results and Savitsky's empirical formulas for wake profile, (a) FnL = 1.89, (b) FnL = 3.34

different Froude numbers are compared with experimental results in Figure 6. This figure shows good agreement between the numerical and experimental results. The average error for wetted keel length, wetted chine length, dynamic sinkage, dynamic trim and drag force are 10.7%, 6.3%, 12.1%, 33.8% and 9.2%, respectively.

The stable positions of the hull, with stern wake profiles at centreline, are illustrated in Figure 7 for Froude numbers 1.89 and 3.34. In the same figure, the calculated wake profiles are compared with Savitsky's formula (Savitsky & Morabito, 2010), which again shows a good agreement.

Results

The numerical results calculated for different step forward swept angles are presented, and the effects of these angles on the hydrodynamic performance of a vessel are investigated and discussed. The calculations were performed for five step angles of 0, 3, 6, 8 and 10 degrees at two Froude numbers, 1.89 and 3.34. In order to create the desired step angle, the
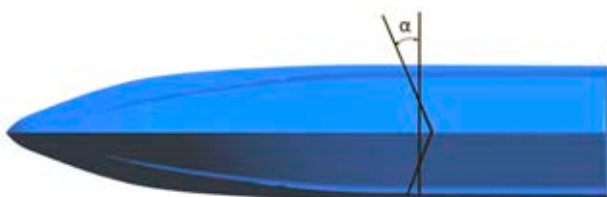
zero-degree step was rotated about the middle point of the half-breadth by α degrees, so that the area of the fore and aft hulls and displacement remained constant. The step forward swept angle of α is illustrated in Figure 8.

Dynamic trim and sinkage

Variations of dynamic trim and sinkage in terms of the step forward swept angle are shown in Figures 9 and 10 for Froude numbers 1.89 and 3.34,
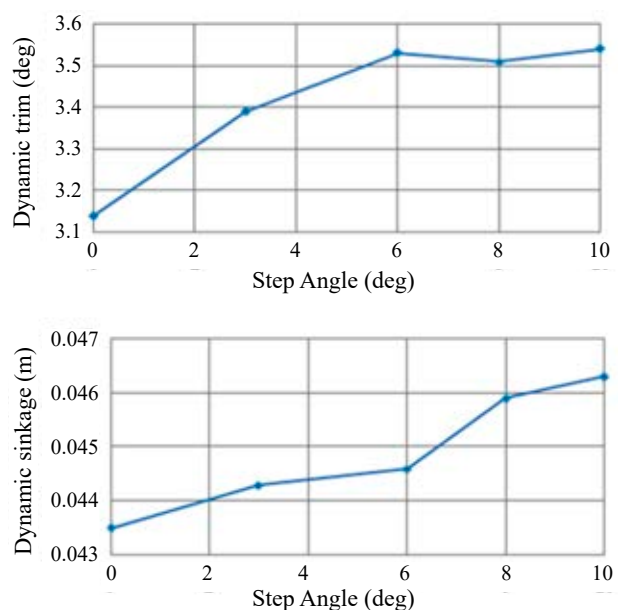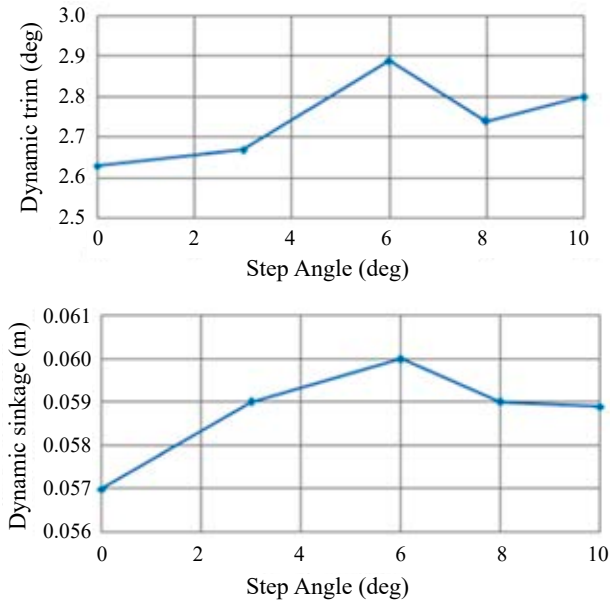

Figure 8. Step forward swept angle of α

Figure 9. Variations of dynamic trim and sinkage in terms of step forward swept angle for Froude number 1.89

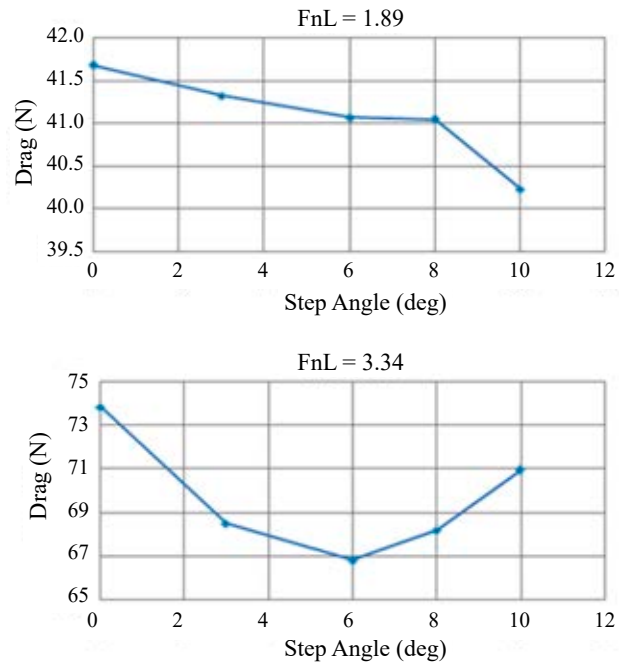**Figure 10. Variations of dynamic trim and sinkage in terms of step forward swept angle for Froude number 3.34**

Figure 11. Variations of drag force with step angle at Froude numbers 1.89 and 3.34
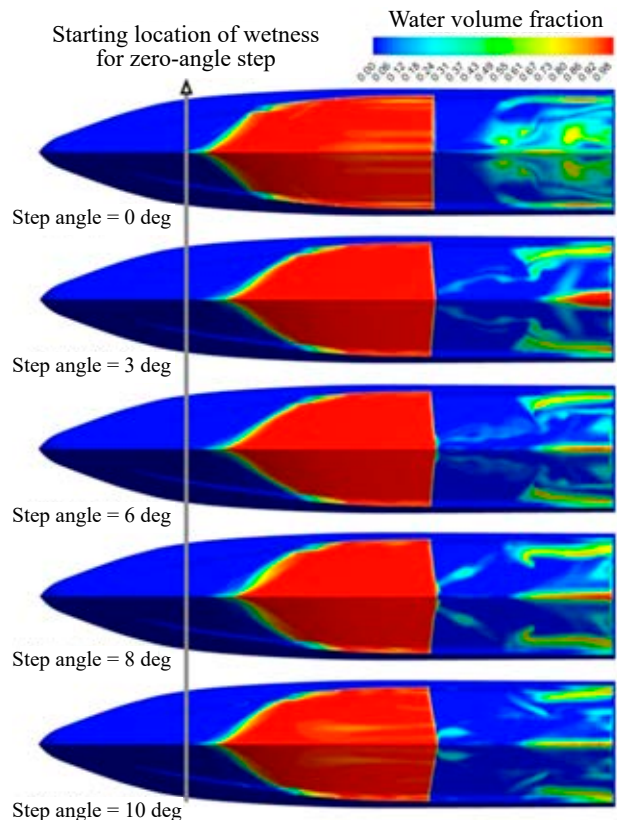
respectively. Generally, it can be seen that the trim and sinkage are increased by increasing the step angle from 0 to 10 degrees for Froude number 1.89. The increase in trim and sinkage are 13% and 6%, respectively. Also, for Froude number 3.34, the trim and sinkage are first increased and then decreased, so that the maximum values of trim and sinkage occur at the angle of 6 degrees. The increase of trim at this angle is 10%, while the increase of sinkage is 5%.

Drag force and wetted surface

In Figure 11, the change in drag force due to step forward swept angle variations is shown for Froude numbers 1.89 and 3.34. It is obvious that the drag reduces with step angle at Froude number 1.89. The minimum drag occurs at a step angle of 10 degrees (a reduction of 3.5% relative to the zero-angle step). Also, for Froude number 3.34, the minimum drag occurs at a step angle of 6 degrees (a reduction of 9.5% relative to the zero-angle step). It is known that the drag is a function of wetted surface area; on the other hand the wetted surface area is a function of the hull position (i.e. dynamic trim and sinkage). Increasing trim and sinkage leads to wetted area reduction, and consequently drag reduction. The variations of drag presented in these figures are therefore consistent with the trim and sinkage diagrams shown in the previous section. The wetted surface area for different step angles at Froude number 3.34 are illustrated in greater detail in Figure 12. It is obvious that the minimum wetted area

Figure 12. Wetted surface areas for different step angles at Froude number 3.34

occurs at a step angle of 6 degrees, corresponding to minimum drag, and the maximum wetted area occurs at a step angle of 0 degrees, corresponding to maximum drag.

Conclusions

The effect of the step forward swept angle on the hydrodynamic performance of a hard chine planing hull was numerically studied. The transient turbulent free surface flow around the hull was modelled by using RANS equations with a standard *k-ε* turbulence model coupled with VOF equations. In addition, rigid body equations for two degrees of freedom were solved in a coupled manner with fluid flow governing equations in order to calculate the heave and pitch motions of the vessel. The presented numerical model was validated against experimental results. Based on the good agreement between numerical and experimental results, it is concluded that the numerical model presented in this study can be used as an accurate model to predict the hydrodynamic performance of hard chine stepped planing hulls. Moreover, the effects of the step forward swept angle on drag are relatively significant, and the angle of step corresponding to minimum drag is dependent on Froude number value, so that a maximum reduction of about 3.5% at a step angle of 10 degrees occurred for FnL = 1.89, and a maximum reduction of about 9.5% at a step angle of 6 degrees for FnL = 3.34.

Acknowledgments

Conflict of interests

The authors declare that there is no conflict of interests regarding the publication of this paper.

References

1. Akkerman, I., Dunaway, J., Kvandal, J., Spinks. J. & Bazilevs, Y. (2012) Toward free-surface modeling of planing vessels: simulation of the Fridsma hull using ALE-VMS. *Computational Mechanics* 50, 6, pp. 719–727.

2. Bakhtiari, M., Veysi, S.T.G. & Ghassemi, H. (2016) Numerical modeling of the stepped planing hull in calm water. *International Journal of Engineering; TRANSACTIONS B: Applications* 29, 2, pp. 236–245.

3. Brizzolara, S. & Serra, F. (2007) *Accuracy of CFD codes in the prediction of planing surfaces hydrodynamic characteristics*. 2nd International Conference on Marine Research and Transportation, Naples.

4. Garland, W.R. & Maki, K.J.A. (2012) Numerical study of a two-dimensional stepped planing surface. *Journal of Ship Production and Design* 28, 2, pp. 60–72.

5. Ghassabzadeh, M. & Ghassemi, H. (2014) Determining of the hydrodynamic forces on the multi-hull tunnel vessel in steady motion. *Journal of the Brazilian Society of Mechanical Sciences and Engineering* 36, 4, pp. 1–12.

6. Ghassemi, H. & Ghiasi, M. (2008) A combined method for the hydrodynamic characteristics of planing craft. *Ocean Engineering* 35, pp. 310–322.

7. Ghassemi, H. & Yumin, S. (2008) Determining the hydrodynamic forces on a planing hull in steady motion. *Journal of Marine Science and Application* 7(3), pp. 147–156.

8. Kazerooni, M.F. & Seif, M.S. (2017) Experimental evaluation of forward speed effect on maneuvering hydrodynamic derivatives of a planing hull. *Scientific Journals of the Maritime University of Szczecin, Zeszyty Naukowe Akademii Morskiej w Szczecinie* 49, 121, pp. 40–53.

9. Kohansal A.R., Ghassemi, H. & Ghiasi, M. (2010) Hydrodynamic characteristics of high speed planing hulls, including trim effect. *Turkish Journal of Engineering and Environmental Sciences* 34, pp. 1–16.

10. Kohansal, A.R. & Ghassemi, H. (2010) A numerical modeling of hydrodynamic characteristics of various planing hull forms. *Ocean Engineering* 37, pp. 498–510.

11. Savitsky, D. (1964) Hydrodynamic design of planing hulls. *Marine Technology* 1, 1, pp. 71–95.

12. Savitsky, D., DeLorme, M.F. & Datla, R. (2007) Inclusion of whisker spray drag in performance prediction method for high-speed planing hulls. *Marine Technology* 44, pp. 35–56.

13. Savitsky, D. & Morabito, M. (2010) Surface wave contours associated with the forebody wake of stepped planing hulls. *Marine Technology* 47, 1, pp. 1–16.

14. Svahn, D. (2009) *Performance prediction of hulls with transverse step*. Master thesis, Marina System Center for Naval Architecture, KTH, Stockholm.

15. Taunton, D., Hudson, D. & Shenoi, R. (2010) Characteristics of a series of high speed hard chine planing hulls. Part 1: performance in calm water. *International Journal of Small Craft Technology* 152, pp. 55–75.

16. Veysi, S.T.G., Bakhtiari, M., Ghassemi, H. & Ghiasi, M. (2015) Toward numerical modeling of the stepped and non-stepped planing hull. *Journal of the Brazilian Society of Mechanical Sciences and Engineering* 37, 6, pp. 1635–1645.

17. Yumin, S., Qington, C., Hailong, S. & Wei, L. (2012) Numerical simulation of a planing vessel at high speed. *Journal of Marine Science and Application* 11, 2, pp. 178–183.